

MICROSCOPIC STUDIES ON VARIOUS SILICON MATERIALS IRRADIATED WITH DIFFERENT HIGH ENERGETIC PARTICLES

M. Kuhnke, E. Fretwurst and G. Lindstroem

*II. Institut für Experimentalphysik, University of Hamburg
Luruper Chaussee 149, DESY Bldg. 67b, D-22761 Hamburg*

ABSTRACT

Phosphorous doped high resistivity silicon materials with different concentrations of the impurities oxygen and carbon were irradiated with 23 GeV protons, 27 MeV protons, 192 MeV pions, neutrons with a mean energy of 5.3 MeV and reactor neutrons. The DLTS-method is used to determine the defect parameters. The introduction rates of the various radiation induced defects depend on the particle type and the impurity concentration. The introduction rates for the point defects VO_i , C_iC_s and C_iO_i are found to be higher for charged particle irradiations. The introduction rate of the divacancy VV is independent on the impurity content and independent on the particle type. The impurities oxygen and carbon influence only the kinetics of point defects. The sum of the introduction rates of mobile primary generated defects silicon self-interstitials I and vacancies V depend only on the particle type. The filling behaviour of the defects VO_i and C_iC_s have been investigated for hadron irradiation in different materials. The filling behaviour of both defects are described well by a exponential time dependence in silicon with a low oxygen content or high carbon content for hadron irradiation, but in oxygen rich silicon the filling behaviour shows a deviation from the theoretical prediction confirmed by a comparison with the filling behaviour after ^{60}Co γ -irradiation.

INTRODUCTION

Silicon detectors are used in the inner tracking region of High Energy Physics experiments, because a high spatial resolution and a fast readout is needed to track the particles. In future experiments the collisions of particles with high energy and

luminosity will lead to intense radiation fields. Hence radiation damage of silicon detectors is a main issue of the future High Energy Experiments [1]. An increase of the leakage current, a change of the effective space charge density [2] and a decrease of charge collection efficiency [3] are well known effects after hadron irradiation. The evolution of the effective space charge density in negative direction from the initial positive value is responsible for the change of the full depletion voltage of silicon detectors. It was shown that oxygen enrichment of silicon have a beneficial effect on the depletion voltage after charged hadron irradiation [4]. This beneficial effect of interstitial oxygen is not observed after neutron irradiation [5].

The reverse current of fully depleted silicon detectors scales linear with the Non Ionisation Energy Loss (NIEL) of high energetic particles and is independent on the impurity content, e.g. oxygen and carbon [6]. It is assumed that the reverse current is dominated by the generation of charge carriers inside the cluster regions [7].

However, microscopic characterisation of radiation induced defects could help to explain the macroscopic results on the scale of defect formation during irradiation and defect evolution after irradiation. The Deep Level Transient Spectroscopy (DLTS) is used to investigate the defect properties [8].

EXPERIMENTAL PROCEDURES

Various silicon materials doped with phosphorous with specific resistivities ranging from $120\Omega cm$ to $2.8k\Omega cm$ and different content of oxygen and carbon were irradiated with neutrons, protons and pions. The concentrations of oxygen and carbon in all investigated samples are several order of magnitudes higher than the phosphorous concentration. The material properties are listed in table 1.

The area of the p^+n junction is $5 \times 5 \text{ mm}^2$ [9]. The thickness of the delivered wafers is about $300 \mu m$. The crystal orientation of all wafer is $\langle 111 \rangle$.

The irradiations have been performed with 23 GeV protons at the PS/CERN [10], 27 MeV at Legnaro/Italy accelerator [11], 192 MeV pions at PSI/Villingen [12]. The neutrons were generated by nuclear reactions in a reactor at Ljubljana/Slovenia [13] or the Be(d,n) reaction at the PTB Braunschweig/Germany [14]. The reactor neutrons have a broad energy spectrum from meV to MeV. The neutrons of the Be(d,n) source have a mean energy of 5.3 MeV.

The equivalent fluence for the 23 GeV proton, 192 MeV pion and reactor neutron irradiations was calculated from the measured reverse current at fully depleted reference diode processed on $10\text{-}20k\Omega cm$ standard FZ. All diodes were heated 80min at $60^\circ C$ to avoid any errors due to different annealing states after irradiation. The Be(d,n) neutron source was employed to determine the current damage constant [2]. The equivalent fluence for the 27 MeV proton irradiation was calculated from the particle fluence and the hardness factor. The equivalent fluences are in the range between $10^{10}\text{-}10^{12} cm^{-2}$.

Most silicon diodes investigated by DLTS were annealed for 80min at $60^\circ C$. Only one time the heating step 4min at $80^\circ C$ was employed. Both heating treatments

Table 1: *Material properties of the investigated samples*

Crystal type	Producer	ρ [Ωcm]	[O] [$10^{16} cm^{-3}$]	[C] [$10^{16} cm^{-3}$]
n-FZ	ITME	120	< 5	≤ 2
n-FZ	ITME	800	17	< 2
n-FZ	ITME	1.2k	21	1
n-FZ	Polovodice	2.8k	< 5	< 1
n-FZ	Polovodice	2.8k	23	< 1
n-FZ	Polovodice	1.5k	< 5	1.8
n-CZ	Polovodice	100	90	0.5
n-FZ	Wacker	400	< 5	< 2
n-FZ	Wacker	10-20k	< 5	< 0.5

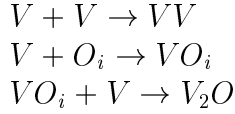
are equivalent. A commercially available DLTS apparatus was used for defect characterization which is described in more detail elsewhere [15]. The displayed spectra correspond to the sinus correlator function and were obtained with a time window of 200 ms. The reverse bias was 10V and during filling with electrons a filling pulse 0V was applied to the diode. During the filling with holes the diode was biased in forward direction. The applied bias voltage was $-3V$. Both filling pulses had a duration of 100 ms.

DEFECT GENERATION AND KINETICS

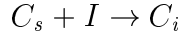
During irradiation of crystalline silicon with high energetic particles some kinetic energy is transferred to silicon atoms of the lattice. The threshold energy to displace a silicon atom out of its lattice sites is about 20 eV. The recoiled silicon atom is called Primary Knock on Atom (PKA). The PKA loses its kinetic energy by displacement of further silicon atoms. The energy loss is mainly at the end of the stopping range of a PKA [16]. PKAs with a energy in the eV range generate mainly isolated point defects and PKAs in the keV range generate clusters. The energy transfer to a PKA depends on the impinging particle type. Therefore mainly clusters are generated in the crystal lattice after hadron irradiation and isolated point defects after electron or γ -photon irradiation.

After the primary generation of silicon self-interstitial I and vacancies V in the crystal lattice a migration of these species at room temperature take place [17]. It is assumed that the recombination rate of interstitials and vacancies is high in the terminal cluster regions, because of the high density of primary generated defects. Other possible reaction are the formation of intrinsic defects like the divacancy VV . In the small cluster regions common impurity atoms like interstitial oxygen O_i and substitutional carbon C_s have no influence on the defect kinetics, because the mean number of an impurity species in a cluster region is small. Hence the defects inside or near the cluster regions are of intrinsic nature. Outside the cluster regions reactions with impurity atoms are possible. A set of reactions is listed below:

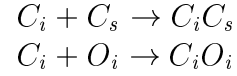
V reactions



I reactions



C_i reactions



The probability of the formation of divacancies outside the cluster regions is small because of the high oxygen concentration in even standard FZ silicon. In the high fluence regime also the defect V_2O is generated. This defect is suggested to be of major importance in defect engineering [18].

Mainly four types of defects are generated in the crystal lattice after high energy particle irradiation in the low fluence regime: the vacancy-interstitial oxygen complex VO_i , the interstitial carbon-substitutional carbon complex C_iC_s , the interstitial carbon-interstitial oxygen complex C_iO_i and the divacancy VV . Other not identified defects with smaller introduction rates have been observed.

EXPERIMENTAL RESULTS

INTRODUCTION RATES - DEPENDENCE ON THE PARTICLE TYPE

The samples of the jet-oxygenated FZ 800/1.2k Ω cm were irradiated with neutrons, protons and pions. The DLTS-spectra of the electron and hole emission from defect centers are shown in figure 1. The corresponding radiation induced

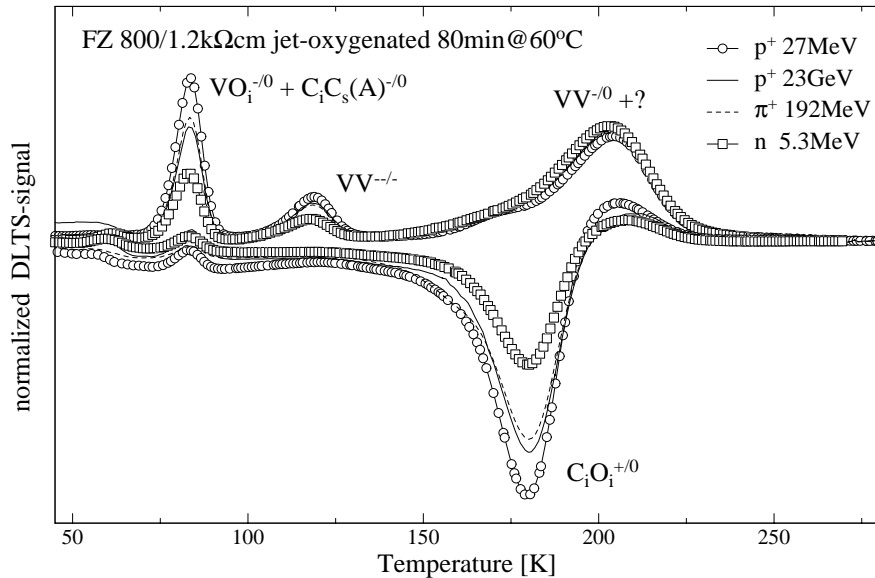


Figure 1: DLTS-spectra of jet-oxygenated FZ 800/1.2k Ω cm samples irradiated with different particles. The DLTS-signals are normalized to NIEL.

defects are assigned to the peaks in the DLTS-spectra. The spectra are normalized to the NIEL of the particles. The introduction rates of the defects VO_i , C_iC_s and C_iO_i depend on the particle type and are higher for charged particles, as shown in

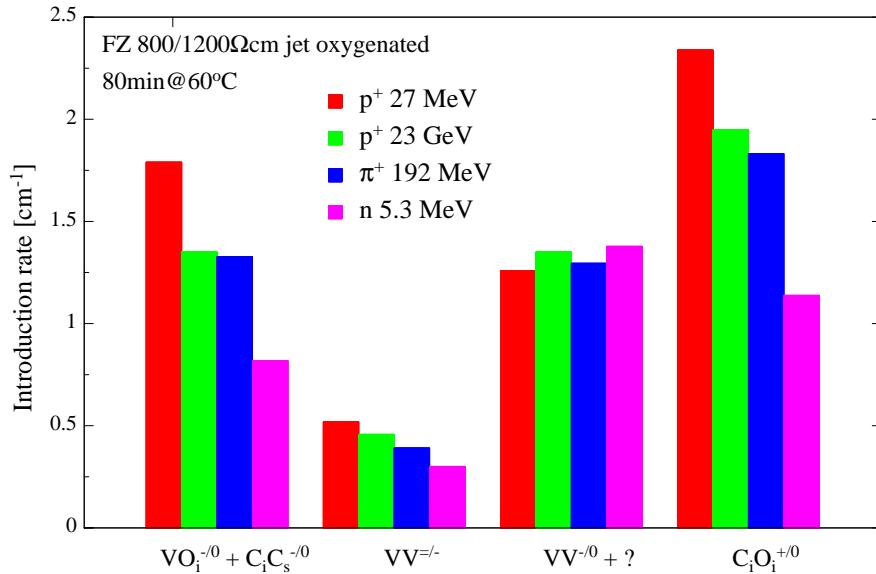


Figure 2: *The introduction rates of radiation induced defects in jet-oxygenated FZ 800/1.2kΩcm samples irradiated with different particles normalized to NIEL.*

figure 2. Also a dependence on the proton energy is visible. The introduction rate of the $VV^{+?}$ is nearly independent on the particle type. The introduction rates of radiation induced defects are summarized in table 2.

The defects VO_i , C_iC_s and C_iO_i are attributed to isolated point defects in the crystal lattice as expected from the unperturbed shape of their DLTS-signal. However, the height and width of the DLTS-signals of the two charge states of the divacancy are different. The signal of the $VV^{=/-}$ is smaller compared to the signal of the $VV^{-/0}$. The ratio of the signals of the both charge states $[VV^{=/-}]/[VV^{-/0}]$ depends on the particle type and energy, as shown in figure 3. This signal ratio is more suppressed for neutron than for the charged particle irradiations. Two different models can explain this effect either due to inter-charge-transfer between the different charge states of divacancy [7] or deformations and strain fields in the crystal lattice [19].

The higher introduction rates of point defects for charged particles can be explained by the enhancement of small energy transfer to PKAs due the coulomb scattering [20]. Thus the beneficial effect of interstitial oxygen on the effective space charge density versus charged hadron fluence can be connected with the higher introduction rate of the point defect V_2O . Macroscopic measurements on oxygenated silicon show a reduction of the depletion voltage of silicon detectors [4]. No or only a weak beneficial effect of oxygen is seen after neutron irradiation [5].

On the other hand the clusters which are associated with divacancies are created by PKAs with a recoil energy in the keV range and nearly no influence of the particle type and energy is seen on the introduction rate of $VV^{+?}$.

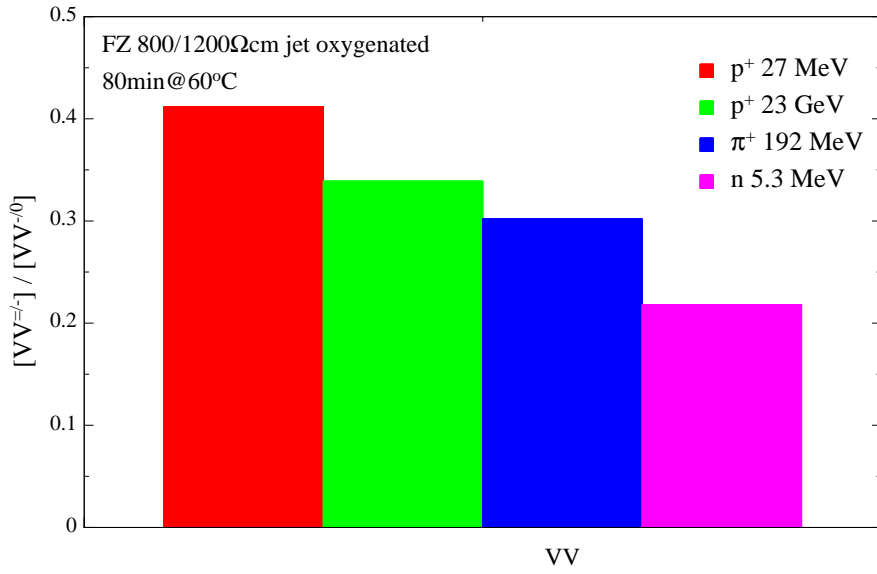


Figure 3: The ratio of the defect concentrations of the two charge states of the divacancy in jet-oxygenated FZ 800/1.2kΩcm samples irradiated with different particles.

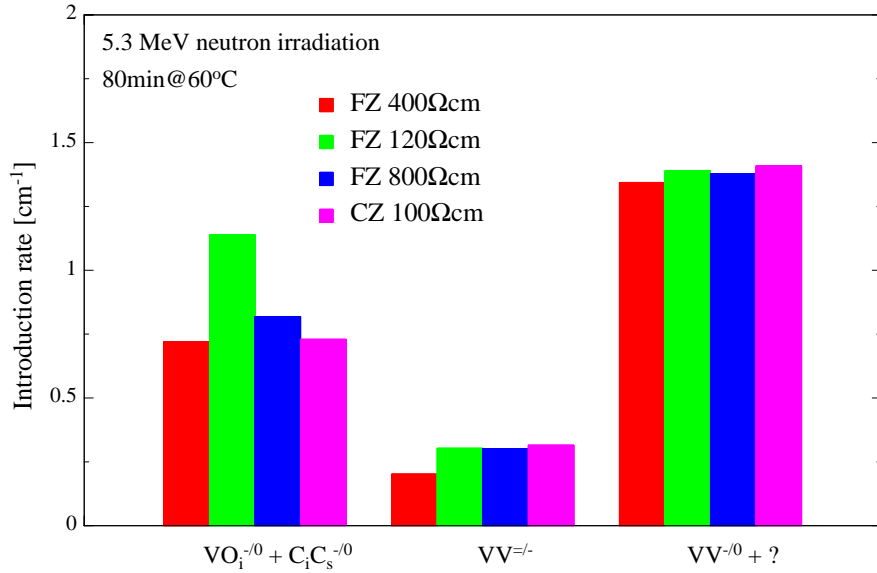


Figure 4: The introduction rates of radiation induced defects in samples of different FZ materials irradiated with 5.3 MeV neutrons normalized to NIEL.

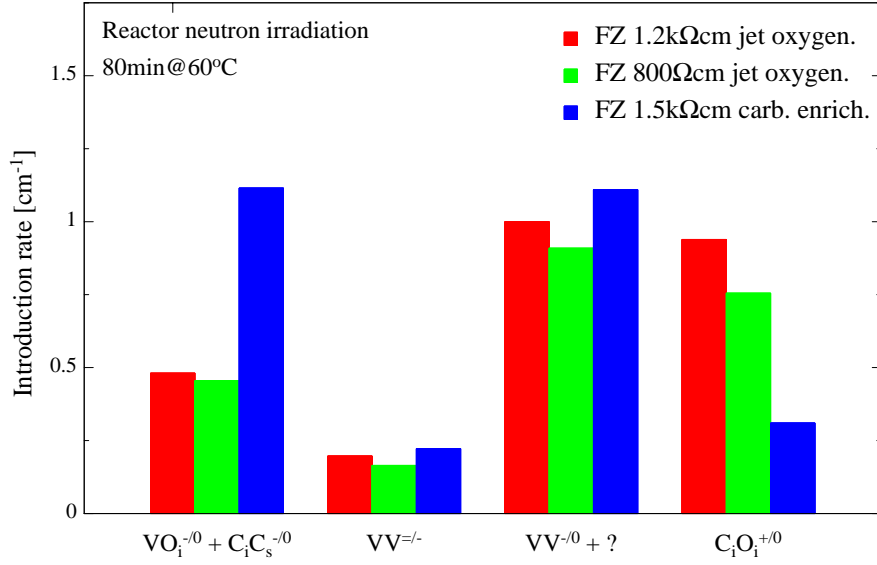


Figure 5: The introduction rates of radiation induced defects in jet-oxygenated FZ 800/1.2kΩcm and carbon enriched FZ 1.5kΩcm samples irradiated with reactor neutrons normalized to NIEL.

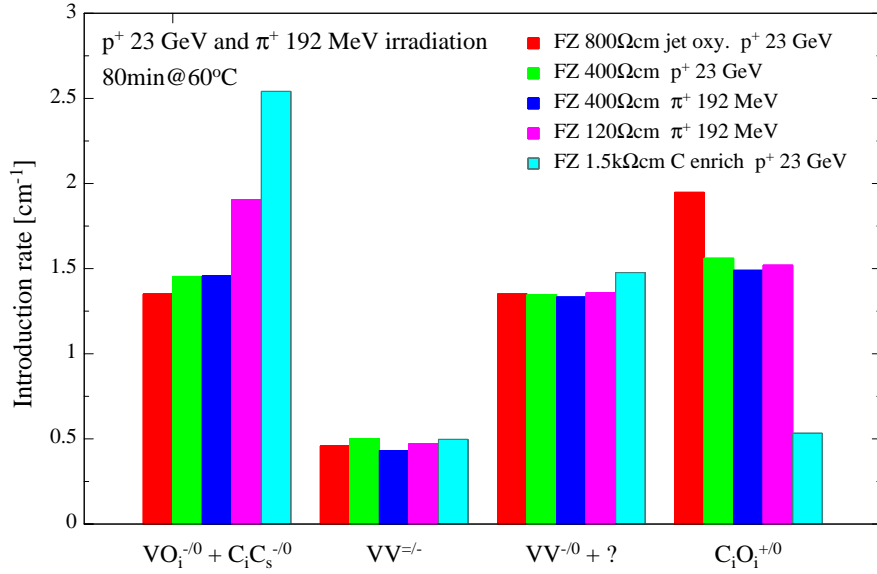


Figure 6: The introduction rates of radiation induced defects in samples of different FZ materials irradiated with 23 GeV protons and 192 MeV pions normalized to NIEL.

Table 2: Introduction rates of radiation induced defects for different particles in jet-oxygenated FZ 800/1.2kΩcm samples.

Particle type	$g(VO_i + C_iC_s)$	$g(C_iO_i)$	$g(VV+?)$
p^+ 27 MeV	1.79 cm^{-1}	2.34 cm^{-1}	1.26 cm^{-1}
p^+ 23 GeV	1.35 cm^{-1}	1.95 cm^{-1}	1.35 cm^{-1}
π^+ 192 MeV	1.33 cm^{-1}	1.83 cm^{-1}	1.30 cm^{-1}
n 5.3 MeV	0.82 cm^{-1}	1.14 cm^{-1}	1.38 cm^{-1}

Table 3: Introduction rates of point defects $g(VO_i + C_iC_s)+g(C_iO_i)+g(C_i)$ for different particles in oxygen and carbon enriched FZ samples.

Particle type	Jet-oxygenated FZ	Carbon enriched FZ
p^+ 23 GeV	3.30 cm^{-1}	3.79 cm^{-1}
n reactor	1.31 cm^{-1}	1.65 cm^{-1}

INTRODUCTION RATES - MATERIAL DEPENDENCE

In figure 4 the material dependence after 5.3 MeV neutron irradiation is shown. Only the sample of FZ 120Ωcm have a higher introduction rate of the defects $VO_i + C_iC_s$. It is suggested that the material has a higher carbon content in comparison to the other materials and therefore the introduction rate of the carbon complex C_iC_s is higher. The same result is also observed after irradiation with reactor neutrons, as shown in figure 5. The introduction rate of both point defects $VO_i + C_iC_s$ is enhanced and the introduction rate of the defect C_iO_i is suppressed in carbon enriched FZ 1.5kΩcm, while in jet-oxygenated FZ 800/1.2kΩcm the generation of the point defects $VO_i + C_iC_s$ is suppressed and the defect C_iO_i generation is enhanced. This behaviour can be explained by sharing of mobile interstitial carbon C_i at O_i and C_s sites.

The material dependence after 23 GeV proton and 192 MeV pion irradiation is shown in figure 6. The samples of FZ 400Ωcm were irradiated with both types of particles and the introduction rates are the same, hence 23 GeV protons and 192 MeV pions generate the same damage in the crystal lattice. Again the sum of the introduction rates of the defects $VO_i + C_iC_s$ is higher in the samples of FZ 120Ωcm and carbon rich FZ 1.5kΩcm. The introduction rate of the defect C_iO_i in the sample of FZ 120Ωcm is conflicting. It should be lower, but however the listed impurity concentrations in table 1 exclude further conclusions and perhaps are not complete.

The sum of the introduction rates of point defects $g(VO_i + C_iC_s)+g(C_iO_i)+g(C_i)$ after 23 GeV proton and reactor neutron irradiation in jet-oxygenated FZ 800/1.2kΩcm and carbon enriched FZ 1.5kΩcm is given in table 3. In conclusion the sum of the introduction rates of the mobile primary generated defects silicon self-interstitials I and single vacancies V depend mainly on the particle type. The dependence on the impurity content in the silicon material is weak.

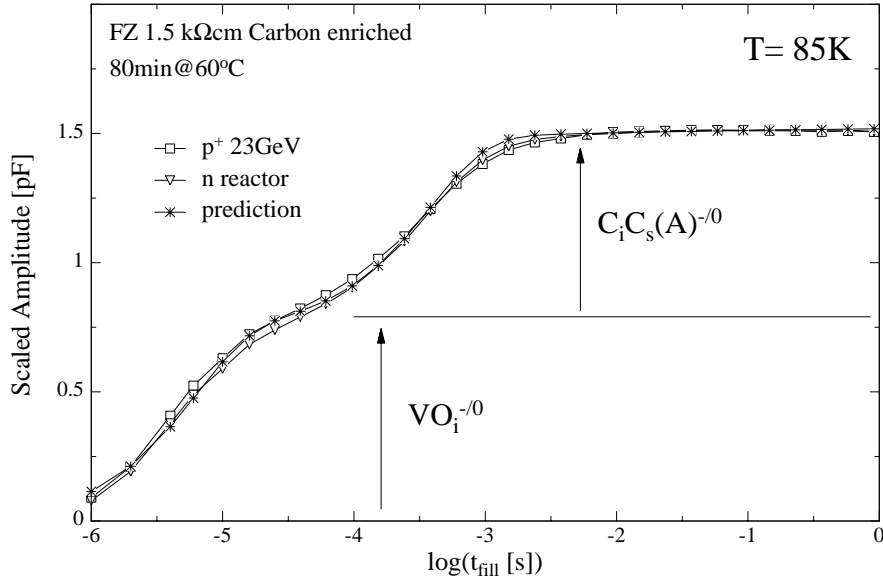


Figure 7: Capture measurements of carbon enriched FZ $1.5k\Omega cm$ samples irradiated with 23 GeV protons and reactor neutrons. The filling behaviour of the two defects VO_i and C_iC_s is shown. The amplitudes are scaled for comparison. Also the theoretical prediction is shown.

CAPTURE MEASUREMENTS

The filling behaviour of the defects VO_i and C_iC_s for the samples of carbon enriched FZ $1.5k\Omega cm$ after 23 GeV proton and reactor neutron irradiation is shown in figure 7. All states of the defect center VO_i are already occupied with majority charge carriers for short filling pulses. The capture time constant of the defect center VO_i is about $6 \mu s$ [21]. The configuration change of the defect $C_iC_s^-(B) \rightarrow C_iC_s^-(A)$ is observed for filling pulses with a longer duration [22]. The signal of C_iC_s in the configuration B is not detected, because of its short emission time constant. Only the portion of C_iC_s in the configuration A is measured. After electron emission C_iC_s change again its configuration $A \rightarrow B$ and the configuration B capture majority charge carriers during applying the filling pulse. The occupied defect state changes its configuration $B \rightarrow A$ with a time constant of about 40 ms at $T=85k$. This observed configuration change is described well by an exponential time dependence.

In the sample of FZ $120\Omega cm$ irradiated with 5.3 MeV neutrons the capture rate of the defect VO_i is not constant, as shown in figure 8. It is suggested that a local high density of negative charged radiation induced defects reduce the free majority charge carrier density during filling. But these explanations are speculative. Even a built-up of a space charge region around the cluster is possible [23].

The filling behaviour of the defects VO_i and C_iC_s after 5.3 MeV neutron irradiation depends on the oxygen concentration, as shown in figure 9. In the sample of FZ $2.8k\Omega cm$ with $[O] < 5 \cdot 10^{16} cm^{-3}$ the deviation of the filling behaviour from the theoretical prediction is small. But in the sample of oxygen enriched FZ $2.8k\Omega cm$ with $[O] = 2.3 \cdot 10^{17} cm^{-3}$ the filling behaviour of both defects is not described by the

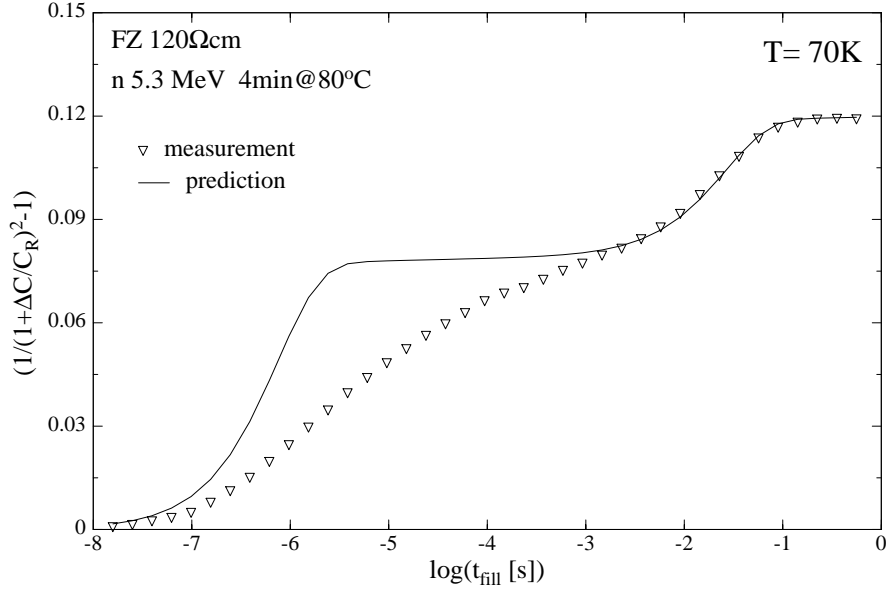


Figure 8: Capture measurement of FZ 120Ωcm sample irradiated with 5.3 MeV neutrons. The filling behaviour of the two defects VO_i and C_iC_s is shown. Also the theoretical prediction is shown.

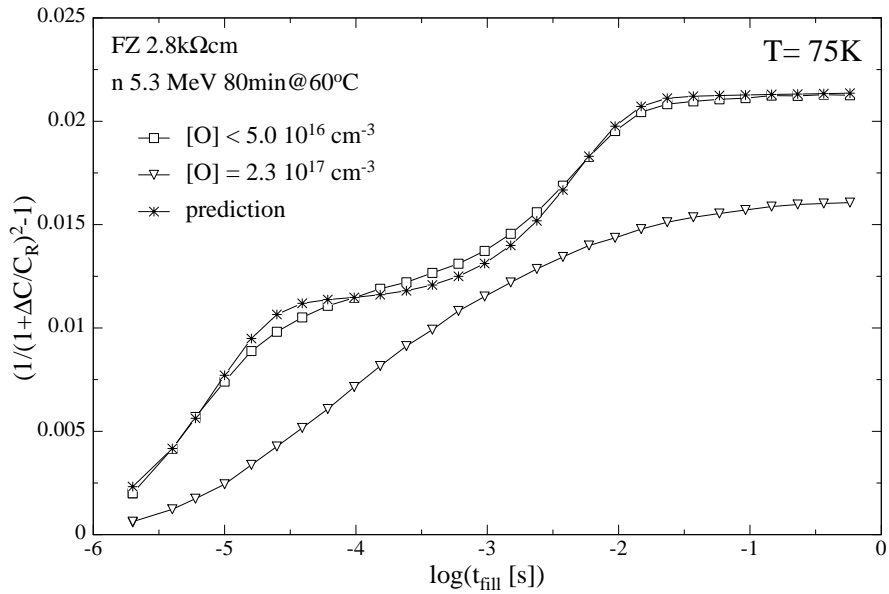


Figure 9: Capture measurements of FZ 2.8kΩcm samples irradiated with 5.3 MeV neutrons. The silicon is enriched with oxygen by high temperature diffusion. The filling behaviour of the two defects VO_i and C_iC_s is shown. Also the theoretical prediction is shown.

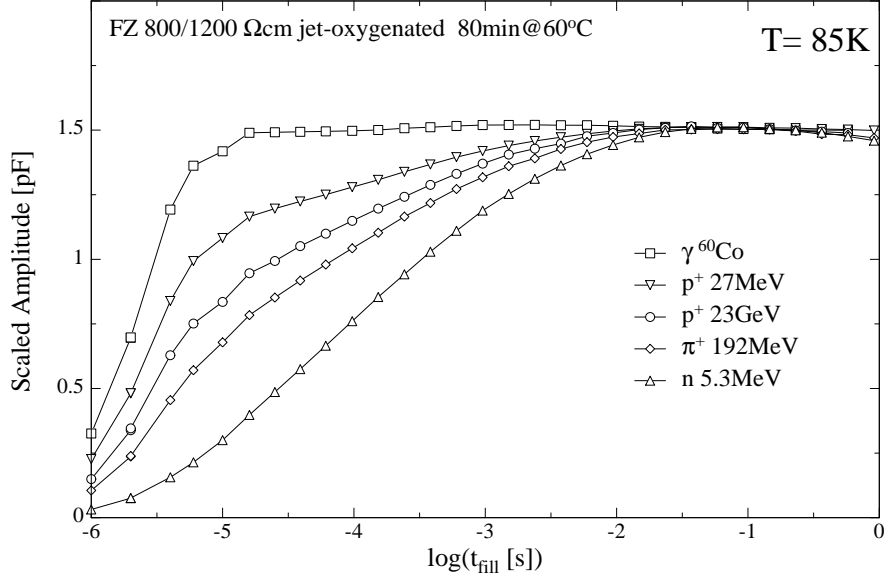


Figure 10: Capture measurements of jet-oxygenated FZ 800/1.2k Ωcm samples irradiated with different particles and γ -photons. The filling behaviour of the two defects VO_i and C_iC_s is shown. The amplitudes are scaled for comparison.

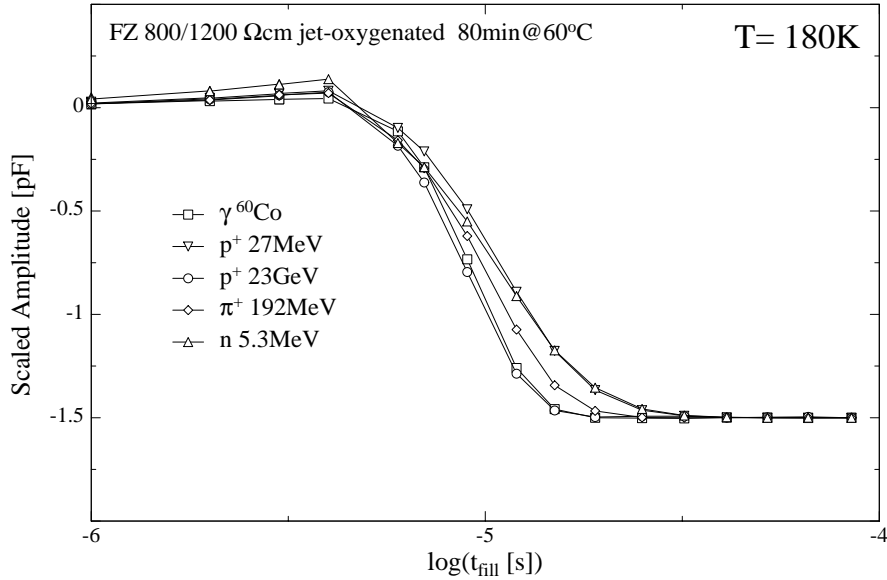


Figure 11: Capture measurements of jet-oxygenated FZ 800/1.2k Ωcm samples irradiated with different particles and γ -photons. The filling behaviour of the defect C_iO_i is shown. The amplitudes are scaled for comparison.

theoretical prediction. Deformations and strain fields originating from the clusters are suggested to change the configuration switching of the defect C_iC_s .

The particle dependence of the filling behaviour of the defects VO_i and C_iC_s in samples of jet-oxygenated FZ 800/1.2kΩcm is shown in figure 10. The filling behaviour of the samples irradiated with hadrons shows a deviation from the filling behaviour of the γ -irradiated sample. The concentration of the defect C_iC_s is very small in oxygen rich silicon after γ -irradiation. The generation rate of the defect C_iC_s seemed to be higher in hadron irradiated samples.

The filling behaviour of defect center C_iO_i filled by forward injection is independent on the particle type in jet-oxygenated FZ 800/1.2kΩcm and no significant difference is seen in comparison to γ -irradiation, as shown in figure 11. The localization of the defect C_iO_i is given by the distribution of its immobile precursor O_i as for the defect VO_i .

SUMMARY

The introduction rates of the point defects VO_i , C_iC_s and C_iO_i depend on the particle type and on the impurity concentrations of oxygen and carbon in the silicon material. Neutron irradiations show the lowest introduction rates of point defects. After charged particle irradiation more point defects are generated than after neutron irradiation. Irradiations with 23 GeV protons and 192 MeV pions have the same introduction rates. Thus the radiation damage of both particle types is assumed to be identical. Irradiations with 27 MeV protons give the highest introduction rates of point defects. This suggests that the coulomb interaction, which produce PKAs with a low recoil energy, is responsible for the enhanced generation of point defects. It is further assumed that the generation of point defects is responsible for the beneficial effect of interstitial oxygen on the effective space charge density of silicon detectors after charged hadron irradiations. A comparison between oxygen and carbon enriched material shows that the sharing of interstitial carbon C_i at substitutional carbon C_s and interstitial O_i sites depends on the oxygen and carbon content. Thus the generation of other defects like V_2O is also influenced by these impurities. The sum of the introduction rates of all three defects VO_i , C_iC_s and C_iO_i suggest that the sum of the introduction rates of mobile primary generated silicon self-interstitials I and vacancies V depend mainly on the particle type and not on the impurity content of the material.

The introduction rate of the divacancy VV is nearly independent on the particle and material type and only lower for reactor neutron irradiations. But the ratio between the signals of the double negatively charge state and the single negatively charge state of VV depends on the particle type. The structure of the cluster damage is assumed to be dependent on the particle type.

Because the 1 MeV neutron equivalent fluence is also calculated from the measured reverse current and the introduction rate of VV is nearly independent on the particle type, the assumption that the volume generation current is proportional to the NIEL is confirmed and the divacancies are related to the cluster damage.

The filling behaviour of the defects VO_i and C_iC_s show a particle and material

dependence. In carbon rich silicon the deviation from the theoretical prediction is small and does not depend on the the particle type. But in oxygen rich silicon the filling behaviour is particle dependent and shows a deviation from the filling behaviour after γ -irradiation. The filling behaviour of the defect C_iO_i is independent on the particle type in oxygen rich silicon and no difference in comparison to γ -irradiation is visible. The formation of the extrinsic defects like VO_i and C_iC_s in the cluster periphery is strongly influence by the impurity content of oxygen and carbon. The switching properties of C_iC_s can be changed by deformations and strain fields originating from the clusters. The free majority charge carrier concentration can be reduced by a high local density of radiation induced defects.

However, it is suggested that the local defect kinetic in the periphery of the clusters is complicated only to be accomplished by simulation programs.

ACKNOWLEDGEMENTS

The authors would like to thank R. Böttger, H.J. Brede and H.Klein for providing the irradiation facility at the Physikalisch-Technische Bundesanstalt Braunschweig, V. Cindro and M. Mikuz for the providing the irradiation facility at the Ljubljana reactor, G. Casse, M. Glaser, F. Lemeilleur, A. Ruzin and A. Zanet for providing the irradiation facility at CERN, K. Gabathuler for providing irradiation facility at PSI-Villingen and D. Bisello and J. Wyss for the exposures at the Legnaro irradiation facility.

Financial support is acknowledged from CERN LHCC to the RD48 collaboration and from the BMBF to our group under contract 05 7HH171.

REFERENCES

1. G. Lindstroem et al. Nucl. Instr. and Meth. **A426** (1999) 1
2. M. Moll: Ph.D. thesis, University of Hamburg (1999)
3. T.J. Brodbeck et al. to be published
4. A. Ruzin et al. Technical Report ROSE/TN/99-5, CERN (1999)
5. A. Ruzin et al. Nucl. Instr. and Meth. **A426** (1999) 94
6. M. Moll et al. Nucl. Instr. and Meth. **A426** (1999) 87
7. K. Gill et al. J.Appl.Phys. **82** (1) (1997) 126 and Erratum J.Appl.Phys. **85** (11) 7990
8. E. Moll et al. Nucl. Instr. and Meth. **A388** (1997) 335
9. M. Wegrzecki et al. 4th ROSE Workshop RD48, December 1998
10. European Laboratory for Particle Physics (CERN), CH-1211 Geneva 23

11. Laboratori Nazionali di Legnaro - Via Romea 4 - 35020 - Legnaro (Padova), Italy
12. Paul Scherrer Institut, CH-5232 Villigen PSI, Switzerland
13. Jozef Stefan Institute, University of Ljubljana, SI-1000 Ljubljana, Slovenia
14. H.J. Brede et al., Nucl. Instr. and Meth. **A274** (1989) 332
15. Dr.L. Cohausz, Halbleitermeßtechnik GmbH, Moosburg
16. G.P. Mueller et al. IEEE **NS-29** (6) (1982) 1493
17. B.C. MacEvoy et al. Nucl. Instr. and Meth. **A374** (1996) 12
18. B.C. MacEvoy et al. Solid State Phenomena Vols. **57-58** (1997) 221
19. B.G. Svensson et al. Phys.Rev **B55** (16) (1997) 10498
20. F. Lemeilleur et al. CERN/LHCC 2000-009 LEB Status Report/RD48 (1999)
21. D. Pons J.Appl.Phys. **55** (10) (1984) 3644
22. L.W. Song et al. Phys.Rev **B42** (9) (1990) 5765
23. B.R. Gossik J. Appl. Phys. **30** (8) (1959) 1214